

Miniature quantum-well microwave spectrometer operating at liquid-nitrogen temperatures

I. V. Kukushkin

Max-Planck-Institut für Festkörperforschung, Heisenbergstrasse 1, D-70569 Stuttgart, Germany
and Institute of Solid State Physics, Russian Academy of Sciences, Chernogolovka, 142432, Russia

S. A. Mikhailov

Mid-Sweden University, ITM, Electronics Design Division, 851 70 Sundsvall, Sweden

J. H. Smet^{a)} and K. von Klitzing

Max-Planck-Institut für Festkörperforschung, Heisenbergstrasse 1, D-70569 Stuttgart, Germany

(Received 23 August 2004; accepted 29 November 2004; published online 18 January 2005)

We demonstrate that a two-dimensional electron system fabricated from a GaAs/AlGaAs quantum well in the presence of a magnetic field B possesses the ability to detect electromagnetic radiation in a broad frequency range. Irradiation of the sample with microwaves produces a dc-photovoltage which oscillates as a function of B . The amplitude and the period of the oscillations are proportional to the radiation power and the wavelength, respectively. Successful operation of such a detector/spectrometer is reported for microwave frequencies up to ~ 150 GHz and temperatures up to ~ 80 K. We do not anticipate any principal difficulties in extending the operation frequency further into the terahertz region. © 2005 American Institute of Physics. [DOI: 10.1063/1.1856143]

Detection of millimeter and submillimeter electromagnetic radiation [frequencies f of 100 GHz to a few terahertz (THz)] remains a challenging applied-physics problem. Schottky diodes,¹ conventionally used in the microwave range, are broadband detectors sensitive to the power of the electromagnetic radiation, but insensitive to its frequency. Their use for measuring the frequency requires complicated schemes including gratings, moving mirrors, or similar elements. Selective and tunable infrared detectors, based on electronic transitions in quantum wells,^{2–5} are free from such disadvantages, but demand very low temperatures for their operation. As they rely on a substantial population difference between two energy levels, such detectors only work properly when $kT \ll \hbar\omega$. This implies $T \approx 10$ K in the infrared and even lower temperatures in the THz and sub-THz frequency ranges. Using not electron but *plasmon* resonances in semiconductor structures can help to circumvent this severe temperature limitation, due to the classical nature of plasma excitations. Voltage tunable detection of radiation by exploiting plasmon resonances in gated submicron field-effect transistors has been proposed in Refs. 6 and 7 and experimentally demonstrated at sub-THz frequencies in Refs. 8–11 (see also Ref. 12). Unfortunately, the use of “standard” two-dimensional (2D) plasmons for the detection of radiation imposes another restriction on the operating conditions of the devices. 2D plasmons are observable only when $\omega\tau > 1$ and the momentum relaxation time $\tau(T)$ essentially decreases with increasing temperature. Hence, the detection of radiation is possible only at sufficiently large frequencies and sufficiently low temperatures. In practice, detection of $f = 600$ GHz radiation was possible only at $T = 8$ K.^{10,11} The need for transistors with very short gate lengths (150 nm^{10,11}) represents another complication of the 2D plasmon detection scheme.

In this letter, we report on the detection of radiation by GaAs/AlGaAs quantum-well devices under the conditions $kT \gg \hbar\omega$ and $\omega\tau \lesssim 1$. The samples had the shape of standard Hall bars with dimensions on the millimeter scale and with several pairs of potential probes on each side of the channel. They were placed in a perpendicular field B . Microwave radiation (20 GHz $\lesssim f \lesssim 150$ GHz) induced a dc voltage between any pair of potential probes on the same side of the Hall bar (photoresistance oscillations have been observed too¹³). This photovoltage was periodic in B . The oscillation amplitude and period were proportional to the microwave power and the wavelength, respectively. Hence, the effect can be used for the detection and spectroscopy of electromagnetic radiation.

Operation of our devices is based on the excitation of a special class of plasma waves in the two-dimensional electron system (2DES): *edge magnetoplasmons* (EMPs). A recent review is found in Ref. 14. EMPs are plasma waves localized near and propagating along the edge of the 2DES in a direction determined by the orientation of the external B field. If the applied B field satisfies the condition $\omega_c\tau > 1$, they are observable at both large and small values of $\omega\tau$ ¹⁵ (experimental observation of EMPs at $\omega\tau \approx 10^{-6}$ has been reported in Ref. 16). Here, ω_c is the cyclotron frequency. EMPs can be excited by microwaves in the vicinity of the contacts [see left inset to Fig. 1(c)] or near any other “irregularities” violating the translational invariance of a straight-line edge, such as for instance indentations or protrusions [right inset to Fig. 1(c)]. The external ac electric field induces an oscillating dipole moment near the contact, which serves as an antenna emitting EMPs. Two or more contacts, separated a distance L apart, emit EMPs coherently. This results in a complicated interference pattern of the EMP field inside the device. Dependent on the parameter $m = qL/2\pi$, interference may either be constructive [$m = \text{integer}$, Fig. 1(a)] or destructive [$m = \text{integer} + 1/2$, Fig. 1(b)], where q is the EMP wave vector. The EMP-field oscillations are then rectified by nonlinear behavior in the contacts, so that in the end a dc

^{a)}Electronic mail: j.smet@fkf.mpg.de

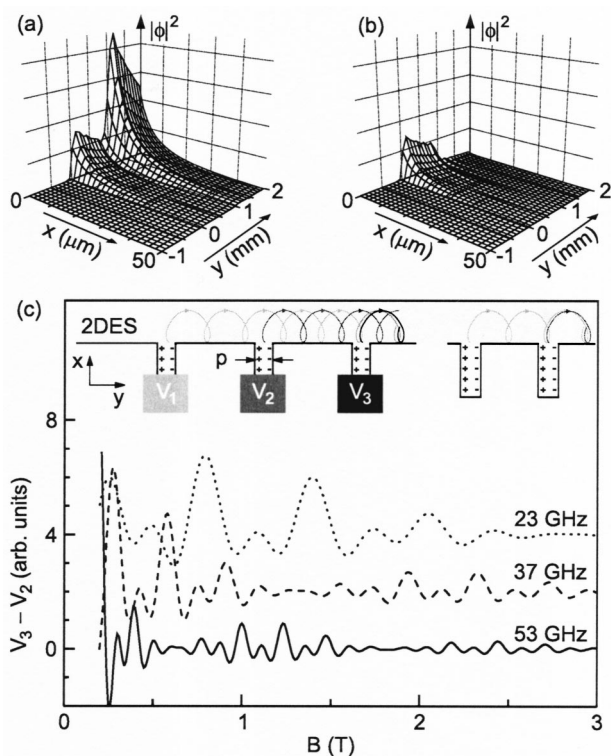


FIG. 1. Examples of the calculated (a) constructive and (b) destructive interference of EMPs emitted by a pair of contacts placed at the edge of the 2DES ($x=0$) 1 mm apart along the y axis at $y=0$ and $y=1$ mm. Here, ϕ is the EMP potential. The density and mobility of the 2D electrons are $n_s = 2.6 \times 10^{11} \text{ cm}^{-2}$ and $\mu = 3 \times 10^6 \text{ cm}^2/\text{V s}$; the frequency f equals 53 GHz. (c) The calculated microwave induced dc voltage, which appears between a pair of potential probes for various frequencies and a sample with $n_s = 2.5 \times 10^{11} \text{ cm}^{-2}$, $\mu = 1.6 \times 10^6 \text{ cm}^2/\text{V s}$, $L = 0.5$ mm, and a potential probe width $p = 0.1$ mm. It is assumed that there are three potential contacts along the side of the Hall bar. The EMPs propagate in the direction from contact 1 to contact 3. The dc voltage V_j at the j th contact is taken proportional to $|\phi(x=0, y_j)|^2$ and the voltage $V_3 - V_2$, shown on the plot, develops between contacts 2 and 3. Curves are shifted vertically for clarity. Insets schematically illustrate the distribution of microwave-induced charges near the contacts where EMPs are emitted.

voltage develops between different pairs of contacts. It oscillates as a function of qL . Since for EMPs $q \propto \omega B/n_s$ —Ref. 15 (n_s is the electron density), the photovoltage oscillates as B is swept with a period $\Delta B \propto n_s/fL$ (for a more accurate analysis of the periodicity see Ref. 13). Figure 1(c) shows some examples of calculated B -field dependencies of the photovoltage for typical experimental parameters.

All samples were processed from the same GaAs/AlGaAs heterostructure into Hall-bar geometries with a width W of either 0.4 or 0.5 mm and with a distance between adjacent potential probes L of 1.6, 0.5, 0.4, 0.2, or 0.1 mm. The electron concentration and mobility (at 4 K) varied from 1.6 to $3.3 \times 10^{11} \text{ cm}^{-2}$ and 0.6 to $1.3 \times 10^6 \text{ cm}^2/\text{V s}$, respectively. The sample was placed in an oversized 16 mm waveguide at the maximum of the microwave electric field. Microwave generators covered the frequency range from 12 to 158 GHz. Further experimental details can be found in Ref. 13.

Figures 2(a) and 2(b) display the B -field dependence of the microwave induced photovoltage measured for microwave frequencies of 40 and 55 GHz and distance $L = 0.5$ mm. The amplitude of the photovoltage oscillations is nearly insensitive to temperature T in the range 1–20 K. A

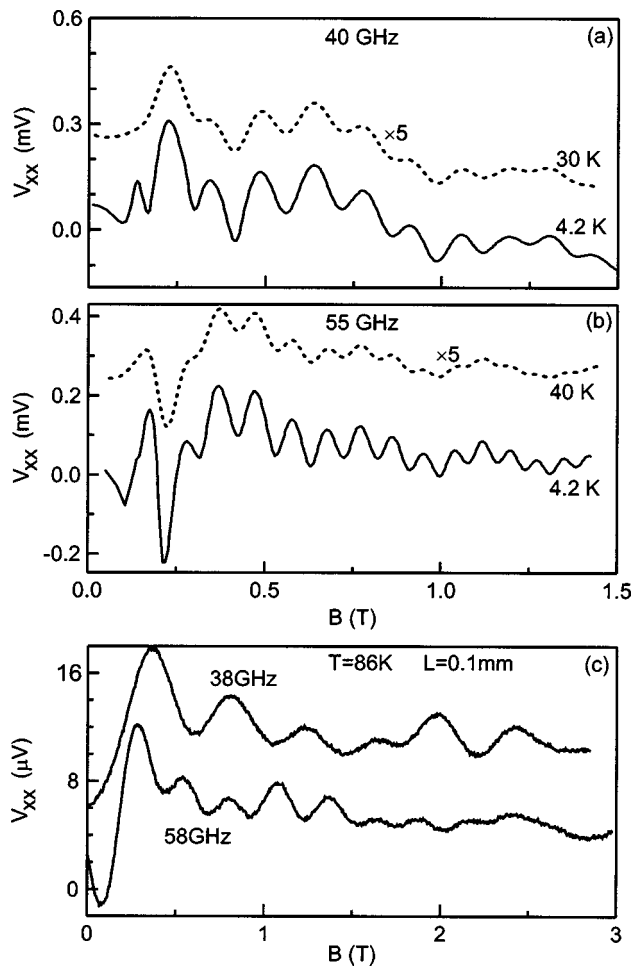


FIG. 2. Magnetic field dependence of the microwave induced photovoltage for (a) $f=40$ GHz and (b) $f=55$ GHz for two different temperatures and 300 μW incident power at the entrance of the microwave waveguide. The electron density is $2.55 \times 10^{11} \text{ cm}^{-2}$ and $L = 0.5$ mm for both plots. (c) Microwave induced photovoltage V_{xx} vs B field at $T = 86$ K for two different frequencies and $L = 0.1$ mm.

further increase of T up to 40 K suppresses the oscillation amplitude by a factor 2–7, dependent on f and the dimensions of the device. For smaller device dimensions, the oscillations were detectable even at $T > 80$ K as illustrated in Fig. 2(c) for $L = 0.1$ mm. Figure 3(a) shows the T dependence of the peak amplitude in the fast Fourier transform (FFT) of the photovoltage, measured for a small-size device ($L = 0.2$ mm) under 55 GHz radiation. As $\Delta B \propto 1/f$, the FFT directly reveals the spectrum of the incident radiation. Figure 3(b) depicts FFT spectra of the photovoltage under monochromatic and bichromatic radiation. These traces demonstrate not only that the FFT-peak position on the $1/B$ axis is proportional to the radiation frequency, but also that the spectral resolution of these devices is approximately equal to 5 GHz. This is far better compared to other semiconductor based spectroscopy techniques (e.g., using InSb Landau level spectroscopy). At frequencies between 50 and 100 GHz, the effect was detectable down to an input power level of less than 5 nW (at 4 K) when using lock-in detection. In devices having contact pairs separated by unequal distances, oscillations with several periods occur for monochromatic incident radiation. At higher T and f , the larger period oscillations associated with the contact pairs with shorter distances become dominant. This observation is likely related to the re-

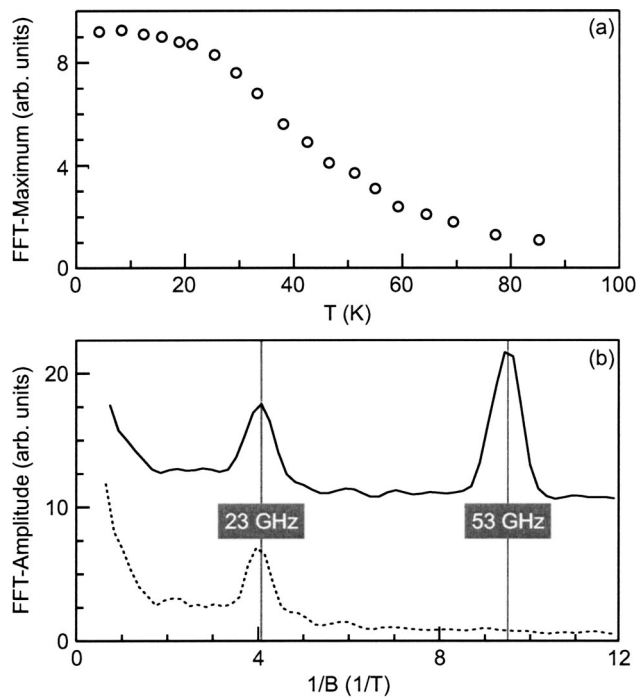


FIG. 3. (a) Temperature dependence of the amplitude of the peak in the FFT of the photovoltage for a device with $L=0.2$ mm and $f=55$ GHz. (b) FFT spectra of the photovoltage when 23 GHz radiation is incident on the sample (bottom curve) or when bichromatic radiation of 23 and 53 GHz illuminates the device (top curve).

duction of the EMP scattering length and requires further studies.

In summary, we have demonstrated the existence of a B -periodic microwave induced ($20 \text{ GHz} \lesssim f \lesssim 150 \text{ GHz}$) photovoltaic effect in GaAs/AlGaAs quantum well devices. It can be exploited for measuring both the frequency and the intensity of incident radiation. The magnetic field plays a dual role. It is responsible for the existence of chiral edge magnetoplasmons and causes the interference inside our small device. Only a moderate magnetic field is needed and it replaces more cumbersome and expensive external interferometric systems. There is no apparent principle difficulty in extending the operating frequency by one order of magni-

tude up to 1 THz and beyond, although it calls for devices with a ten times shorter distance between the contacts. As in our devices L was $\sim 0.1\text{--}0.5$ mm, no submicron technology is needed even at $f \geq 1$ THz.

The authors acknowledge financial support from the Max-Planck and Humboldt Research Grant, the Russian Fund of Fundamental Research, INTAS, and the BMBF through a young investigator award on Nanotechnology.

¹T. W. Crow, R. J. Matlack, R. M. Weikle, and U. V. Bhaskar, in *Compound Semiconductor Electronics*, edited by M. Shur (World Scientific, Singapore, 1996).

²S. G. Matsik, M. B. M. Rinzan, A. G. U. Perera, H. C. Liu, Z. R. Wasilewski, and M. Buchanan, *Appl. Phys. Lett.* **82**, 139 (2003).

³D. G. Esaev, M. B. M. Rinzan, S. G. Matsik, A. G. U. Perera, H. C. Liu, B. N. Zvonkov, V. I. Gavrilenko, and A. A. Belyanin, *J. Appl. Phys.* **95**, 512 (2004).

⁴M. Sherwin, US Patent 5,914,497, 1999.

⁵M. Wraback, P. Shen, and M. Dutta, US Patent 6,476,596, 2002.

⁶M. I. Dyakonov and M. Shur, *IEEE Trans. Electron Devices* **43**, 380 (1996).

⁷M. Dyakonov and M. S. Shur, in *Terahertz Sources and Systems*, NATO Science Series II. Mathematics, Physics and Chemistry, Vol. 27, edited by R. E. Miles, P. Harrison, and D. Lippens (Kluwer, Dordrecht, 2001), pp. 187–207.

⁸J.-Q. Lü and M. S. Shur, *Appl. Phys. Lett.* **78**, 2587 (2001).

⁹W. Knap, V. Kachorovskii, Y. Deng, S. Rumyantsev, J.-Q. Lü, R. Gaska, M. S. Shur, G. Simin, X. Hu, M. Asif Khan, C. A. Saylor, and L. C. Brunel, *J. Appl. Phys.* **91**, 9346 (2002).

¹⁰W. Knap, Y. Deng, S. Rumyantsev, J.-Q. Lü, M. S. Shur, C. A. Saylor, and L. C. Brunel, *Appl. Phys. Lett.* **80**, 3433 (2002).

¹¹W. Knap, Y. Deng, S. Rumyantsev, and M. S. Shur, *Appl. Phys. Lett.* **81**, 4637 (2002).

¹²X. G. Peralta, S. J. Allen, M. C. Wanke, N. E. Harff, J. A. Simmons, M. P. Lilly, J. L. Reno, P. J. Burke, and J. P. Eisenstein, *Appl. Phys. Lett.* **81**, 1627 (2002).

¹³I. V. Kukushkin, M. Y. Akimov, J. H. Smet, S. A. Mikhailov, K. von Klitzing, I. L. Aleiner, and V. I. Fal'ko, *Phys. Rev. Lett.* **92**, 236803 (2004).

¹⁴S. A. Mikhailov, in *Edge Excitations of Low-Dimensional Charged Systems*, edited by O. Kiricsek (Nova Science, New York, 2000), Chap. 1, pp. 1–47.

¹⁵V. A. Volkov and S. A. Mikhailov, *Zh. Eksp. Teor. Fiz.* **94**, 217 (1988) [*Sov. Phys. JETP* **67**, 1639 (1988)].

¹⁶P. J. M. Peters, M. J. Lea, A. M. L. Janssen, A. O. Stone, W. P. N. M. Jacobs, P. Fozzooni, and R. W. van der Heijden, *Phys. Rev. Lett.* **67**, 2199 (1991).